International Journal of Biological Sciences
ISSN 1449-2288 www.biolsci.org 2008 4(6):387-396

Research Paper

LGI1 and LGI4 bind to ADAM22, ADAM23 and ADAM11

Koji Sagane[1,2] ✉, Yasushi Ishihama[1,*], Hachiro Sugimoto[2]

1. Tsukuba Research Laboratories, Eisai Co., Ltd., Tokodai 5-1-3, Tsukuba, Ibaraki 300-2635, Japan.
2. Department of Neuroscience for Drug Discovery, Graduate School of Pharmaceutical Sciences, Kyoto University, Kyoto 606-8501, Japan.

* Present address: Institute for Advanced Biosciences, Keio University, Daihoji, Tsuruoka, Yamagata 997-0017, Japan.

✉ Correspondence to: Koji Sagane, Tsukuba Research Laboratories, Eisai Co., Ltd., Tokodai 5-1-3, Tsukuba, Ibaraki 300-2635, Japan, Tel: +81-29-847-7119, Email: k-sagane@hhc.eisai.co.jp

Received: 2008.05.01; Accepted: 2008.10.20; Published: 2008.10.21

The transmembrane protein ADAM22 is expressed at high levels in the brain. From its molecular structure, ADAM22 is thought to be an adhesion molecule or a receptor because it has functional disintegrin-like and cysteine-rich sequences in its ectodomain. The phenotypic analysis of ADAM22-deficient mice has indicated the important roles played by ADAM22 in proper neuronal function and peripheral nerve development, however, the precise molecular function of ADAM22 is still unknown. To understand the function of ADAM22 on a molecular basis, we identified ADAM22 binding proteins by using immunoprecipitation and mass spectrometric analysis. This analysis revealed that Leucine-rich glioma inactivated 1 (LGI1) is the most potent ADAM22 binding protein in mouse brain. By our quantitative cell-ELISA system, we demonstrated the specific binding of LGI1 with ADAM22. Furthermore, we showed that LGI4, a putative ADAM22 ligand, also bound to ADAM22. Characterization of the binding specificity of LGI1 and LGI4 suggested that ADAM22 is not a sole receptor, because ADAM11 and ADAM23 had a significant binding ability to LGI1 or LGI4. Therefore, LGI-ADAM system seems to be regulated not only by the affinity but also by the cell-type-specific expression of each protein. Our findings provide new clues to understand the functions of LGI1 and LGI4 as an ADAMs ligand.

Key words: ADAM22, ADAM23, LGI1, LGI4, GeLC-MS

INTRODUCTION

A Disintegrin And Metalloprotease (ADAM) is a family of membrane-spanning multi-domain proteins containing a metalloproteinase-like domain and a disintegrin-like domain. Already, more than 30 ADAMs have been identified in mammals. Some types of ADAM are catalytically active metalloproteases and they control receptor-mediated signals by activating membrane-bound growth factors or by shedding the ectodomain of cell-surface receptors [1,2]. ADAMs are also involved in cell-cell or cell-matrix adhesion through their interaction with integrins or syndecans. More than 10 ADAMs have been shown to support integrin-mediated cell adhesion *in vitro* [3]. An analysis of knockout mice has revealed the physiological roles of ADAM family proteins in fertilization, myogenesis and neurogenesis [4,5].

We have reported our findings on ADAM11, ADAM22 and ADAM23 genes and their restricted expression in the nervous system [6,7]. Sequence analysis suggests that they are not metalloproteases, since they all lack a catalytic motif. Recently, we revealed that ADAM11 is essential for a proper neuronal function because ADAM11-deficient mice showed deficits in special learning, motor coordination and nociceptive response [8,9]. Furthermore, we have reported that mice with a truncated mutation of ADAM22 exhibited ataxia, seizure and hypomyelination in the peripheral nerves [10]. It has been reported that the disruption of the *Adam23* gene in mice results in premature death associated with ataxia and tremor [11]. These findings indicate that these three ADAMs are non-redundant and have distinct functions.

In this study, we identified LGI1 as a specific binding partner of ADAM22 protein from mouse brain, and demonstrated the specific interaction between LGI1 and ADAM22 by employing a quantitative cell-ELISA assay. We also showed that LGI4 binds to ADAM22 as well. In addition, characterization of the binding specificity of LGI1 and LGI4 revealed that ADAM22 is not a sole receptor for them. Our results suggest that LGI-ADAM system is more complicated than initially thought.

MATERIALS AND METHODS

Experimental Animals

All the animal procedures conformed to Japanese regulations on the care and use of animals. Moreover, the procedures were in accordance with the Guideline for Animal Experimentation of the Japanese Association for Laboratory Animal Science, and were approved by the Animal Care and Use Committee of Eisai Co., Ltd. Male C57/BL6 mice were purchased from Charles River Japan (Tokyo, Japan).

Antibodies

The rabbit anti-ADAM22-cyto polyclonal antibody was created in our laboratory [10]. The anti-FLAG-M2 mouse monoclonal antibody and anti-HA11 mouse monoclonal antibody were purchased from SIGMA (MO, USA) and Covance (NJ, USA), respectively.

Immunoprecipitation

C57/BL6 mice were sacrificed and their whole brains were quickly removed, frozen in liquid nitrogen, and stored at -80 °C. Each mouse brain was homogenated with a Polytron homogenizer in 5 ml of TN buffer (50 mM Tris-HCl, pH 7.4, 150 mM NaCl, 1 % NP-40) containing protease inhibitor cocktail (Roche Diagnostics, Mannheim, Germany). To remove debris, the homogenates were centrifuged at 15,000g for 5 min, and the resulting supernatants were cleared by 0.45 μm filtration. Anti-ADAM22-cyto antibody (4 μg) were added to 1.6 ml of cleared brain homogenate and incubated for 60 min at room temperature, followed by incubation with 100 μl of Protein-G Agarose (Roche Diagnostics, Mannheim, Germany). The agarose beads were washed three times with TN buffer, and then the bound proteins were eluted in 100 μl of 1.25x SDS-PAGE sample buffer at 95 °C. As a negative control, rabbit normal IgG was used instead of anti-ADAM22-cyto antibody.

Immunoblot and Silver Stain Analysis

The samples were separated on 10 % SDS-PAGE, and transferred to a nitrocellulose membrane. The blot was then incubated with anti-ADAM22-cyto antibody (0.4 μl/ml), and visualized with HRP-conjugated anti-rabbit IgG and an ECL-Plus chemiluminescence detection system (GE Healthcare, NJ, USA). Silver staining was performed using Silver Stain Kit (Daiichi Pure Chemicals, Tokyo, Japan) according to the manufacturer's instructions.

Protein Identification of 60 kDa Gel Band by Mass Spectrometry

The target gel band at 60 kDa and the corresponding band of the negative control were excised after silver staining. In-gel digestion was performed in the presence of Cymal-5 according to the protocol described by Katayama et al. [24]. After being desalted using StageTips [25], each sample was analyzed with a nanoLC-MS system consisting of a Finnigan LTQ mass spectrometer (Thermo Fisher Scientific, Bremen, Germany), a Dionex Ultimate3000 pump with an FLM-3000 flow manager (Germering, Germany) and an HTC-PAL autosampler (CTC Analytics, Zwingen, Switzerland). ReproSil-Pur C18 materials (3 μm, Dr. Maisch, Ammerbuch, Germany) were packed into a self-pulled needle (150 mm length x 100 μm I.D., 6 μm opening) to prepare an analytical column needle [26] The injection volume was 5 μL and the flow rate was 500 nL/min. The mobile phases consisted of (A) 0.5 % acetic acid and (B) 0.5 % acetic acid and 80 % acetonitrile. A two-step linear gradient of 5 % to 30 % B in 15 min, 30 % to 100 % B in 5 min and 100 % B for 10 min was used. A spray voltage of 2400 V was applied. The MS scan range was m/z 300-1500 and the top ten precursor ions were selected for subsequent MS/MS scans. A Mass Navigator v1.2 (Mitsui Knowledge Industry, Tokyo, Japan) was used to create peak lists on the basis of the recorded fragmentation spectra. Peptides and proteins were identified by Mascot v2.1 (Matrix Science, London) against UniProt/SwissProt v54.0 with a precursor mass tolerance of 2.0 Da, a fragment ion mass tolerance of 0.8 Da, rodent taxonomy, and strict trypsin specificity allowing for up to 1 missed cleavage. The carbamidomethylation of cysteine was set as a fixed modification, and methionine oxidation was allowed as a variable modification. Peptides were considered identified if the Mascot score was over the 95 % confidence limit based on the 'identity' score of each peptide, and at least two peptides per protein were observed for protein identification. The protein content was calculated based on the emPAI values [13]. Briefly, the number of observed precursor ions per protein was normalized by the number of observable peptides per protein. Then, these normalized values were converted to exponential values so that they were proportional to the protein abundance. The emPAI calculation was performed automatically using a script called emPAI Calc (http://empai.iab.keio.ac.jp/).

Affinity Purification of mouse ADAM22 complex

The ADAM22-matrix was constructed by coupling 50 μg of anti-ADAM22-cyto antibody with 500 μl of AminoLink gel (PIERCE, IL, USA) according to the manufacturer's instructions. In the same way, normal rabbit IgG was used to construct the Negative-matrix. Brain homogenates obtained from one-third of a single brain were incubated with 55 μg

of ADAM22-matrix or Negative-matrix for 60 min at room temperature. The matrixes were washed three times in TN buffer, then the bound proteins were eluted in 60 µl of 2x SDS-PAGE sample buffer at 95 °C. To obtain the final test samples with a 1x SDS concentration, the eluted samples were diluted with an equal amount of distilled water. These test samples were then subjected to immunoblot analysis, silver staining and GeLC-MS analysis.

GeLC-MS Analysis

After separation by SDS-PAGE (5-20 %, 0.5 mm thickness), entire lanes were cut out, sliced into 4 pieces, digested and desalted as described above. Each slice was analyzed with nanoLC-MS as described earlier except for the gradient condition where 5 % to 10 % B in 5 min, 10 % to 30 % B in 60 min, 30 % to 100 % B in 5 min and 100 % B for 10 min were used. The Mascot database searching against UniProt/SwissProt v54.0 was done for each sample and the obtained results were merged to allow a comparison of the ADAM22-immunoprecipitated sample and the negative control. The emPAI Calc script was used to estimate protein abundance.

Plasmid Construction

3.1M-mADAM22: Mouse ADAM22-A04 (alpha-form) cDNA was subcloned into the pcDNA3.1-vector (Invitrogen, CA, USA). 3.1M-hAD11-FG, 3.1M-hAD22a-FG, 3.1M-hAD23-FG: The cDNAs encoding human ADAM11, ADAM22-alpha, ADAM23 tagged with the FLAG epitope (DYKDDDDK) at the C-terminus were subcloned into the pcDNA3.1-vector. 3.1M-mLGI1-HA, 3.1M-mLGI4-HA: Mouse LGI1 and LGI4 cDNAs were amplified from mouse brain Quick-Clone cDNA (Clontech, CA, USA) with a FastStart High Fidelity PCR System (Roche Diagnostics, Mannheim, Germany). The amplified DNA fragments were cloned into the pT7Blue-vector (Novagen, WI, USA). After sequence verification, each cDNA was tagged with the HA epitope (YPYDVPDYA) at the C-terminus, and subcloned into the pcDNA3.1-vector.

Cell-based ELISA

HeLa cells were cultured in RPMI-1640 medium with 10 % calf serum, and plated onto a 96-well cell culture plate one day before transfection. Two plasmids (0.1 µg each) were mixed and cotransfected to the HeLa cells using Lipofectamine2000 reagent (Invitrogen, CA, USA). After a 48 hr incubation, the cells were washed twice with D-PBS (SIGMA, MO, USA), and fixed in 4 % paraformaldehyde (Wako Pure Chemicals, Osaka, Japan) for 15 min. To detect cell surface HA-epitope, the cells were immediately transferred to the blocking step without permeabilization. Instead, when detecting the total amount of FLAG-epitope, the cells were permeabilized with 0.1 % TritonX-100 for 15 min, followed by blocking. Blocking was performed using 1x Blockace solution (Dainippon Pharmaceutical, Osaka, Japan) for 30 min at room temperature. The cells were incubated with primary antibodies (anti-HA; 1:500 dilution, anti-FLAG; 1:1000 dilution) for 30 min, and then washed three times with TBST (50 mM Tris-HCl pH 7.4, 500 mM NaCl, 0.05 % Tween20). After being washed, the cells were incubated with HRP-conjugated sheep anti-mouse-IgG antibody (GE Healthcare, NJ, USA) in a 1:1000 dilution for 30 min and then washed three times. The cell-bound secondary antibodies were detected using TMB substrate solution (KPL, MD, USA). The colorimetric reaction was stopped by the addition of the TMB Stop solution (KPL, MD, USA) and the resulting plates were measured at 450 nm absorption with a SUNRISE microplate reader (Tecan Japan, Kanagawa, Japan).

RESULTS

Isolation of ADAM22 binding proteins from mouse brain

To isolate ADAM22 binding proteins from mouse brain, we performed immunoprecipitation experiments using anti-ADAM22-cyto antibody, which recognizes the cytoplasmic region of human and mouse ADAM22 protein. First, the immunoprecipitates of anti-ADAM22-cyto antibody from mouse whole brain were examined by immunoblot analysis. As shown in Figure 1A, ADAM22 proteins were highly concentrated by this immunoprecipitation (lane 3). On the other hand, no ADAM22 protein was detected in the immunoprecipitates of normal rabbit antibody (lane 5). ADAM22 proteins were observed as multiple bands with molecular weights of 70 to 90 kDa. These multiple bands are thought to be proteins translated from splicing variants, because a wide variety of ADAM22-transcripts have been reported in mice [10,12]. Second, the protein composition of ADAM22-immunoprecipitates (sample #3) and negative-IP-control (sample #5) were analyzed by silver staining (Figure 1B). A strong band with a molecular weight of approximately 60 kDa (arrow in Figure 1B) was observed in the ADAM22-immunoprecipitates but not in the negative control, suggesting that this 60-kDa protein is a specific binder of ADAM22. Mass spectrometry analysis revealed that the most abundant protein (68.7 %) in this 60 kDa band was Leucine-rich glioma inactivated-1 (LGI1) based on the emPAI score, which is derived from the number of observed peptides per protein and is proportional to

protein abundance [13]. The predicted molecular weight of mouse LGI1 is approx 63 kDa, which is consistent with the mobility in our SDS-PAGE analysis.

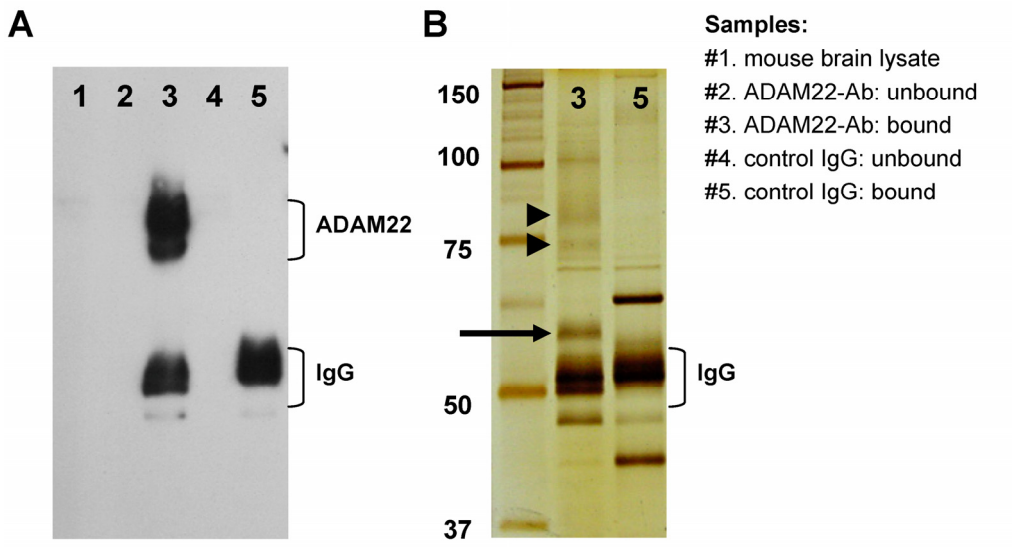

C

Entry name	No. of Peptides	Content (%)*	Description
LGI1_MOUSE	8	68.7	Leucine-rich glioma-inactivated protein 1 precursor
K2C5_MOUSE	3	16.7	Keratin, type II cytoskeletal 5
KCRU_MOUSE	2	14.7	Creatine kinase, ubiquitous mitochondrial precursor

D

Entry name	Sequence	PeptScore
LGI1_MOUSE	SQDLPYQSLSIDTFSYLNDEYVVIAQPFTGK	54
LGI1_MOUSE	GNTQIYK	51
LGI1_MOUSE	DNALCENAR	44
LGI1_MOUSE	TVPPDVISLSFVR	44
LGI1_MOUSE	NFLFASSFK	42
LGI1_MOUSE	GNAFNCDCK	42
LGI1_MOUSE	CIFLEWDHVEK	37
LGI1_MOUSE	KPNDIETFK	35

Figure 1. Immunoprecipitation of ADAM22 from mouse brain. A) Immunoblot analysis. Each sample was examined by immunoblot analysis using anti-ADAM22-cyto antibody. B) Silver stain analysis. Immunoprecipitates of ADAM22-cyto (#3) and control IgG (#5) were examined by silver stain analysis. ADAM22 proteins are indicated by arrowheads and the 60-kDa specific band is indicated by an arrow. C) Mass spectrometric analysis. Protein list of the identified proteins in 60 kDa band of ADAM22-immunoprecipitates. *Content (%) was calculated using emPAI values. D) Identified peptides assigned mouse LGI1. PeptScore is the Mascot peptide score for each peptide in identification.

GeLC-MS analysis of ADAM22-IP-complex

Comparative GeLC-MS analysis [14] is a good way to obtain information about the composition profile of a protein complex. However, when we used immobilized protein-G and primary antibody for the purification, a large amount of IgG coeluted in the immunoprecipitate sample sometimes prevents effective protein detection. To overcome this problem, we made two types of affinity matrixes, which were covalently linked by rabbit anti-ADAM22-cyto antibody (ADAM22-matrix) or control rabbit IgG (negative-matrix), respectively. Both matrixes were incubated with cleared homogenate obtained from mouse whole brain, washed thoroughly and eluted with a solution containing denaturing agents. As shown in Figure 2A, effective purification of ADAM22-complex was accomplished by using the ADAM22-matrix. Figure 2B indicates the decrease in the amount of IgG in sample #7 with keeping the 60 kDa-binding protein (arrow). We performed GeLC-MS analysis and identified 133 and 162 proteins for samples #7 and #9, respectively. Table 1 shows 133 proteins identified from the ADAM22-matrix, and these proteins are plotted by the number of identified peptides for the

ADAM22-matrix and the negative-matrix (Figure 2C). This graph clearly shows that ADAM22 and LGI1 were specifically bound to the ADAM22-matrix among the 133 proteins.

Table 1. Comparative GeLC-MS analysis. 133 proteins identified for sample #7 (ADAM22-matrix bound proteins) were arranged according to the numbers of unique peptides observed with GeLC-MS analysis. For each protein, the numbers of observed peptides for sample #9 (negative-matrix bound proteins) are also indicated.

Entry name	Observed Peptides		Description
	AD22(#7)	Nega(#9)	
ADA22_MOUSE	30	0	ADAM 22 precursor
SPTA2_MOUSE	25	30	Spectrin alpha chain, brain
K2C5_MOUSE	24	18	Keratin, type II cytoskeletal 5
AINX_MOUSE	22	19	Alpha-internexin
K1C14_MOUSE	20	15	Keratin, type I cytoskeletal 14
TBB2A_MOUSE	19	31	Tubulin beta-2A chain
CLH_MOUSE	17	30	Clathrin heavy chain
ACTB_MOUSE	17	28	Actin, cytoplasmic 1
LGI1_MOUSE	16	0	Leucine-rich glioma-inactivated protein 1 precursor
NFL_MOUSE	15	23	Neurofilament light polypeptide
AT1A3_MOUSE	15	20	Sodium/potassium-transporting ATPase subunit alpha-3
SPTB2_MOUSE	15	19	Spectrin beta chain, brain 1
NFM_MOUSE	14	25	Neurofilament medium polypeptide
MYH10_MOUSE	12	32	Myosin-10
TBB2C_MOUSE	9	15	Tubulin beta-2C chain
K2C6A_MOUSE	8	8	Keratin, type II cytoskeletal 6A
K1C17_MOUSE	8	4	Keratin, type I cytoskeletal 17
ATPA_MOUSE	7	13	ATP synthase subunit alpha, mitochondrial precursor
KPYM_MOUSE	7	6	Pyruvate kinase isozymes M1/M2
KCC2A_MOUSE	7	6	Calcium/calmodulin-dependent protein kinase type II alpha chain
AATM_MOUSE	7	6	Aspartate aminotransferase, mitochondrial precursor
AT1A2_MOUSE	6	10	Sodium/potassium-transporting ATPase subunit alpha-2 precursor
MAP1B_MOUSE	6	8	Microtubule-associated protein 1B
MAP1A_MOUSE	6	6	Microtubule-associated protein 1A
K2C1_MOUSE	6	6	Keratin, type II cytoskeletal 1
NSF_MOUSE	6	5	Vesicle-fusing ATPase
K1C10_MOUSE	6	4	Keratin, type I cytoskeletal 10
NFH_MOUSE	5	22	Neurofilament heavy polypeptide
ATPB_MOUSE	5	16	ATP synthase subunit beta, mitochondrial precursor
HSP7C_MOUSE	5	11	Heat shock cognate 71 kDa protein
ENOA_MOUSE	5	10	Alpha-enolase
DYHC_MOUSE	5	9	Dynein heavy chain, cytosolic
DPYL2_MOUSE	5	9	Dihydropyrimidinase-related protein 2
STXB1_MOUSE	5	6	Syntaxin-binding protein 1
MYH8_MOUSE	5	6	Myosin-8
GLNA_MOUSE	5	5	Glutamine synthetase
PLEC1_MOUSE	5	4	Plectin-1
K1C16_MOUSE	5	4	Keratin, type I cytoskeletal 16
1433G_MOUSE	5	3	14-3-3 protein gamma
PYGM_MOUSE	5	1	Glycogen phosphorylase, muscle form
TBB3_MOUSE	4	15	Tubulin beta-3 chain
ALDOA_MOUSE	4	8	Fructose-bisphosphate aldolase A
1433Z_MOUSE	4	7	14-3-3 protein zeta/delta
MYPR_MOUSE	4	6	Myelin proteolipid protein
KCRB_MOUSE	4	6	Creatine kinase B-type
ACON_MOUSE	4	6	Aconitate hydratase, mitochondrial precursor
TPIS_MOUSE	4	5	Triosephosphate isomerase
MAP2_MOUSE	4	5	Microtubule-associated protein 2
ALBU_MOUSE	4	5	Serum albumin precursor
TBB4_MOUSE	4	4	Tubulin beta-4 chain
AT2B2_MOUSE	4	4	Plasma membrane calcium-transporting ATPase 2
AT2A2_MOUSE	4	2	Sarcoplasmic/endoplasmic reticulum calcium ATPase 2
GNAO2_MOUSE	4	0	Guanine nucleotide-binding protein G(o) subunit alpha 2
DLG1_MOUSE	4	0	Disks large homolog 1
CN37_MOUSE	3	6	2',3'-cyclic-nucleotide 3'-phosphodiesterase
PLAK_MOUSE	3	5	Junction plakoglobin
CMC1_MOUSE	3	5	Calcium-binding mitochondrial carrier protein Aralar1
KCC2B_MOUSE	3	4	Calcium/calmodulin-dependent protein kinase type II beta chain
HXK1_MOUSE	3	4	Hexokinase-1
AT1A1_MOUSE	3	4	Sodium/potassium-transporting ATPase subunit alpha-1 precursor
MDHM_MOUSE	3	3	Malate dehydrogenase, mitochondrial precursor
ALDOC_MOUSE	3	3	Fructose-bisphosphate aldolase C
ODPA_MOUSE	3	2	Pyruvate dehydrogenase E1 component subunit alpha, somatic form, mitochondrial precursor
K2C8_MOUSE	3	2	Keratin, type II cytoskeletal 8
HS90A_MOUSE	3	2	Heat shock protein HSP 90-alpha
BASP_MOUSE	3	2	Brain acid soluble protein 1
1433T_MOUSE	3	2	14-3-3 protein theta
ODO2_MOUSE	3	1	Dihydrolipoyllysine-residue succinyltransferase component of 2-oxoglutarate dehydrogenase complex,
K2C4_MOUSE	3	1	Keratin, type II cytoskeletal 4
1433E_MOUSE	3	1	14-3-3 protein epsilon
PRDX2_MOUSE	3	0	Peroxiredoxin-2
EF1A1_MOUSE	3	0	Elongation factor 1-alpha 1
ADT2_MOUSE	3	0	ADP/ATP translocase 2
G3P_MOUSE	2	10	Glyceraldehyde-3-phosphate dehydrogenase
SNIP_MOUSE	2	9	p130Cas-associated protein
TBB5_MOUSE	2	6	Tubulin beta-5 chain
SYN1_MOUSE	2	6	Synapsin-1
MYO5A_MOUSE	2	5	Myosin-Va
HS90B_MOUSE	2	5	Heat shock protein HSP 90-beta
VDAC1_MOUSE	2	4	Voltage-dependent anion-selective channel protein 1
DHSA_MOUSE	2	4	Succinate dehydrogenase [ubiquinone] flavoprotein subunit, mitochondrial precursor
DHE3_MOUSE	2	4	Glutamate dehydrogenase 1, mitochondrial precursor
CAPZB_MOUSE	2	4	F-actin-capping protein subunit beta
MBP_MOUSE	2	3	Myelin basic protein
AP2B1_MOUSE	2	3	AP-2 complex subunit beta-1
PHB2_MOUSE	2	2	Prohibitin-2
KCRU_MOUSE	2	2	Creatine kinase, ubiquitous mitochondrial precursor
K2C1B_MOUSE	2	2	Keratin, type II cytoskeletal 1b
K1C19_MOUSE	2	2	Keratin, type I cytoskeletal 19
G6PI_MOUSE	2	2	Glucose-6-phosphate isomerase
CH60_MOUSE	2	2	60 kDa heat shock protein, mitochondrial precursor
VATH_MOUSE	2	1	Vacuolar ATP synthase subunit H
SUCB1_MOUSE	2	1	Succinyl-CoA ligase [ADP-forming] beta-chain, mitochondrial precursor
SFXN3_MOUSE	2	1	Sideroflexin-3
SEPT5_MOUSE	2	1	Septin-5
KRT85_MOUSE	2	1	Keratin type II cuticular Hb5
KI21B_MOUSE	2	1	Kinesin-like protein KIF21B
K1H1_MOUSE	2	1	Keratin, type I cuticular Ha1
H4_MOUSE	2	1	Histone H4
GRP78_MOUSE	2	1	78 kDa glucose-regulated protein precursor
DLG2_MOUSE	2	1	Disks large homolog 2
CAZA2_MOUSE	2	1	F-actin-capping protein subunit alpha-2
AP180_MOUSE	2	1	Clathrin coat assembly protein AP180
AMPH_MOUSE	2	1	Amphiphysin
AATC_MOUSE	2	1	Aspartate aminotransferase, cytoplasmic
1433B_MOUSE	2	1	14-3-3 protein beta/alpha
SV2A_MOUSE	2	0	Synaptic vesicle glycoprotein 2A
RL13_MOUSE	2	0	60S ribosomal protein L13
PYGB_MOUSE	2	0	Glycogen phosphorylase, brain form
MYL6_MOUSE	2	0	Myosin light polypeptide 6
MARCS_MOUSE	2	0	Myristoylated alanine-rich C-kinase substrate
K1C15_MOUSE	2	0	Keratin, type I cytoskeletal 15
H14_MOUSE	2	0	Histone H1.4

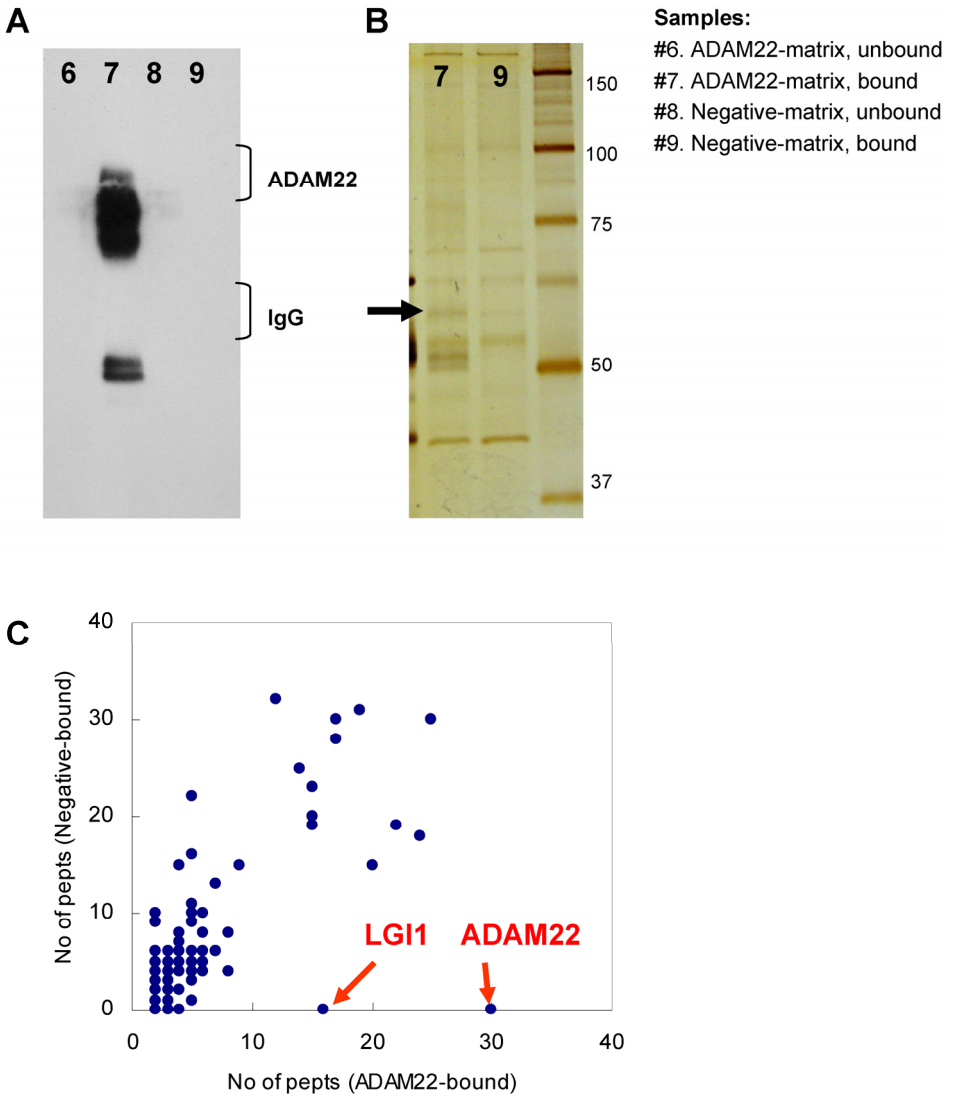

Figure 2. Comparative GeLC-MS analysis for ADAM22-matrix bound proteins and negative-matrix bound proteins. A) Immunoblot analysis. Each sample was examined by immunoblot analysis using anti-ADAM22-cyto antibody. B) Silver stain analysis. The 60-kDa specific band is indicated by an arrow. Note that the amount of IgG was greatly decreased in sample #9. C) The number of identified peptides for 113 proteins from the ADAM22-matrix sample (x-axis) is plotted against that from the negative-matrix sample (y-axis). These 113 proteins are listed in Table 1.

Interaction between ADAMs and LGI1 protein

The LGI1 protein is a secreted protein and ADAM22 is a type I transmembrane protein expressed on the cell surface. Therefore the interaction between these two molecules must occur outside the cell. To determine this interaction, we established a quantitative cell-based ELISA system by using the mouse HA-tagged LGI1 protein (LGI1-HA) and the anti-HA monoclonal antibody. As shown in Figure 3, the amount of cell-bound HA signal was elevated only when it was co-expressed with mouse ADAM22, suggesting that mouse LGI1-HA proteins bind to mouse ADAM22 protein in a specific manner. We next examined the binding specificity of LGI1 in relation to ADAM11, ADAM22 and ADAM23. As these ADAMs share similar sequences in the ectodomain, ADAM11 and ADAM23 were also strong LGI1 receptor candidates. To achieve an accurate normalization, we made assay plates in duplicate. Then we measured one plate for a cell-bound HA signal without permeabilization and examined the other plate for the total expression of ADAMs by FLAG detection under a permeabilized condition. As shown in Figure 4A, the strongest interaction was observed between mouse LGI1 and ADAM23. There was a moderate interaction for ADAM22 and a weaker interaction for ADAM11. Af-

ter normalization with ADAM expression (Figures 4B), ADAM23 exhibited a strong interaction capacity comparable to that of ADAM22. In contrast, ADAM11 was less active than the others (43.3%). These results suggest that ADAM22 is not a sole receptor for LGI1.

Interaction between ADAMs and LGI4 protein

The LGI4 protein is another candidate ligand for ADAM22 receptor. This is because disruption of the *Lgi4* gene in mice causes hypomyelination in the peripheral nerves and this phenotype is quite similar with that of the ADAM22 knockout mice. To address this hypothesis, we examined interaction between mouse LGI4 and mouse ADAM22 proteins by the cell-ELISA analysis. As shown in Figure 5, the significant amount of cell-bound LGI4-HA signal was detected only when it was co-expressed with mouse ADAM22, suggesting that mouse LGI4-HA proteins bind to mouse ADAM22 in a specific manner. We next examined the binding specificity of LGI4 for ADAM11, ADAM22 and ADAM23. Figure 6A shows that the strongest interaction was observed between mouse LGI4 and ADAM22. There was a moderate interaction for ADAM11 and ADAM23. These results suggest that LGI4 interacts with not only ADAM22 but also ADAM11 and ADAM23.

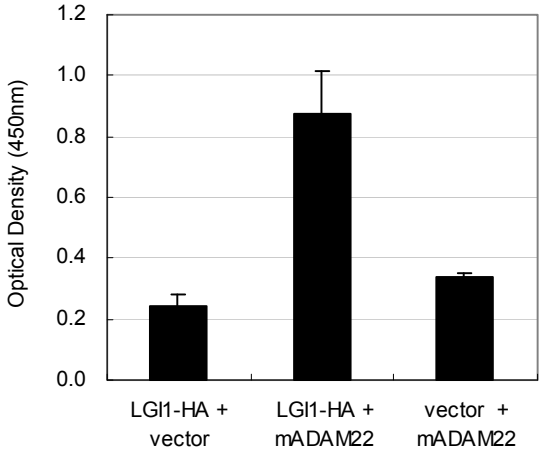

Figure 3. Interaction of mouse LGI1-HA with mouse ADAM22. Cell-bound mouse LGI1-HA proteins were quantified with a cell-based ELISA system. An elevated amount of LGI1-HA was detected only when mouse ADAM22 was co-transfected. Each bar represents the mean ± SEM (n = 4 wells).

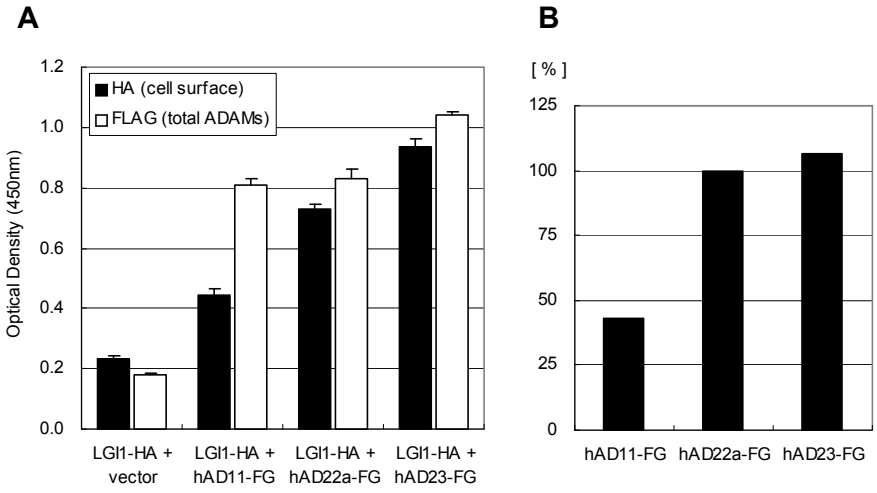

Figure 4. Binding specificity of LGI1-HA against ADAM11, ADAM22 and ADAM23. A) Cell-bound mouse LGI1-HA proteins (black) and total ADAMs-FLAG (white) were quantified with a cell-based ELISA system. Each bar represents the mean ± SEM (n = 4 wells). B) Mean values of the HA signal (cell-bound mouse LGI1-HA) were normalized by ADAMs (FLAG signal).

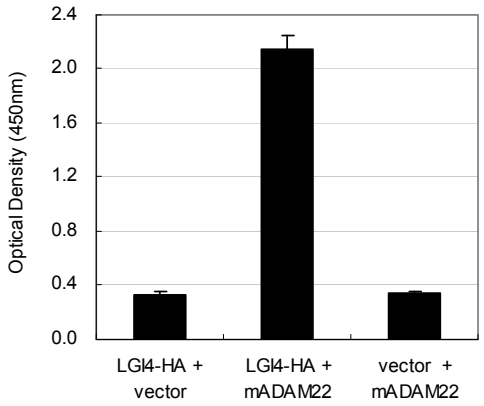

Figure 5. Interaction of mouse LGI4-HA with mouse ADAM22. Cell-bound mouse LGI4-HA proteins were quantified with a cell-based ELISA system. An elevated amount of LGI4-HA was detected only when mouse ADAM22 was co-transfected. Each bar represents the mean ± SEM (n = 4 wells).

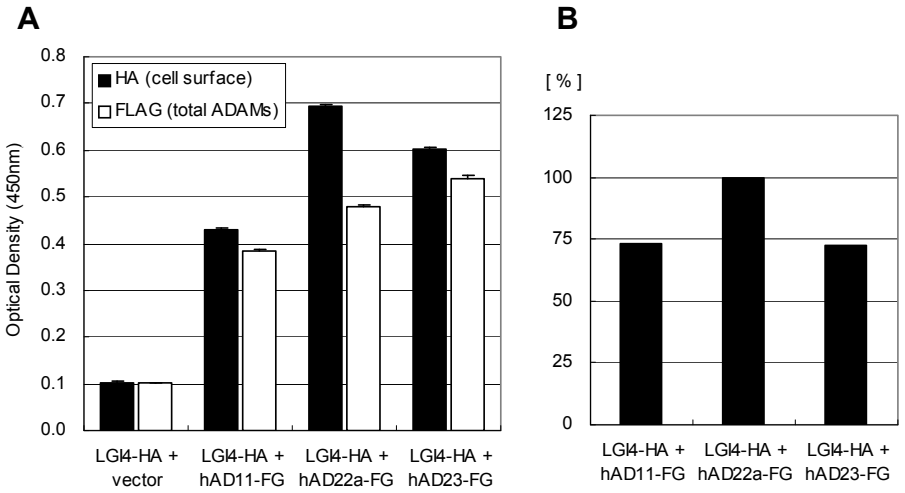

Figure 6. Binding specificity of LGI4-HA against ADAM11, ADAM22 and ADAM23. A) Cell-bound mouse LGI4-HA proteins (black) and total ADAMs-FLAG (white) were quantified with a cell-based ELISA system. Each bar represents the mean ± SEM (n = 4 wells). B) Mean values of the HA signal (cell-bound mouse LGI4-HA) were normalized by ADAMs (FLAG signal).

DISCUSSION

In a previous study, we revealed that ADAM22 is a cell-surface receptor predominantly expressed in neuronal tissues [6,7]. We then discovered several defects in ADAM22 deficient mice, including i) a delay in body weight gain, ii) hypomyelinated peripheral nerves, and iii) seizures and short life spans [10]. These results suggest that ADAM22 is essential for the maintenance of proper neuronal functions in mammals, however, little is known about ADAM22 at the molecular level. To elucidate the molecular function of ADAM22, we initiated a ligand-fishing study for ADAM22 protein.

In this study, to obtain ADAM22-specific binder from mouse brain, we performed immunoprecipitation using anti-ADAM22-cyto antibody and mass spectrometry analysis. Our GeLC-MS and emPAI analysis strongly suggested that LGI1 protein binds specifically to ADAM22. By employing a quantitative cell-based ELISA analysis, we demonstrated the specific interaction between LGI1 and ADAM22 on cultured cells.

The *LGI1* gene was initially identified as a candidate tumor suppressor because the inactivation of the *LGI1* gene is frequently observed in glioblastoma cell lines [15]. Later, the striking discovery was reported that the mutations in the *LGI1* gene cause autosomal-dominant partial epilepsy with auditory features (ADPEAF) [16]. Further studies revealed that LGI1 is a secreted protein and most of the mutant LGI1 causing ADPEAF has a secretion defect, suggesting that LGI1 works as a soluble ligand for the unknown receptor [17]. From these data, together with our findings that the homozygous inactivation of the *Adam22* gene causes seizures in mice, it seemed reasonable to speculate that LGI1 inputs the signal via ADAM22 on the cell surface, and an epileptic seizure would be caused by the impairment of LGI1-ADAM22 signaling.

The interaction of LGI1 with ADAM22 was first discovered by the immunopurification of the post-synaptic large complex using anti-PSD-95 antibodies [18]. The complex contained PSD-95, stargazin, ADAM22 and LGI1. Another group undertook the affinity purification of a Kv1 potassium channel complex, and discovered that it contained PSD-95, ADAM22 and LGI1 [19]. As PSD-95 is known to be a scaffold protein for a variety of receptors or ion channels [20], there was a possibility that LGI1 interacted indirectly with ADAM22 through the intermediary PSD-95. In contrast, our GeLC-MS analysis clearly showed that the interaction between LGI1 and ADAM22 is direct. This is probably because our ADAM22-cyto antibody specifically interacted with ADAM22 cytoplasmic domain, which was not covered with PSD-95.

In ADAM22-deficient mice, we observed hypomyelination in the peripheral nerves while CNS myelin was correctly formed [10]. A very similar phenotype was observed in *claw paw* mice and the causative mutation was recently discovered [23]. The authors found that *claw paw* mice have a 225 base pair insertion in *Lgi4* gene, leading to the production of a protein that lacks exon 4. LGI4 is a member of the LGI family and has a sequence similarity with LGI1. Based on this information, another ligand-receptor pair can be identified, namely LGI4 and ADAM22. We exam-

ined this hypothesis by our cell-ELISA systems and discovered that LGI4 strongly interacts with ADAM22.

The next issue is the binding specificity of LGI1 and LGI4 to ADAM11, ADAM22 and ADAM23, because these ADAMs share similar sequences in the ectodomain. By the cell-ELISA assay, we demonstrated that LGI1 binds to ADAM23 strongly as well as ADAM22 and weakly binds to ADAM11, suggesting that ADAM23 is another receptor for LGI1. It is known that ADAM23 is expressed at high levels in the brain [6,21], is localized on the cell surface [22], and is essential for normal brain function because the ADAM23-deficient mice exhibited ataxia, tremor and short life spans [11]. The knockout phenotype of ADAM22 and ADAM23 seems to be similar but we did not observe tremor in our ADAM22-deficient mice. As we know the mRNA expression pattern of ADAM23 is different from that of ADAM22 [6,10], we speculate that ADAM23 works as an LGI1 receptor in the ADAM22-negative cells.

We also showed that LGI4 significantly binds to all of the three ADAMs. These results indicate that ADAM22 is not a sole receptor for LGI4. Despite the significant binding ability with LGI4 and similar expression patterns with ADAM22, we did not observe any myelination defects in ADAM11-deficient mice [8]. These results suggest that ADAM11 is dispensable for the proper myelination step. Since ADAM11 has a very short cytoplasmic domain comparing to ADAM22, ADAM11 may work as a supportive role or a negative regulator. Since there has been no report about the myelin status of the ADAM23-deficient mice, the importance of ADAM23 in the peripheral nerve myelination is yet to be determined.

In summary, our results indicate that LGI1 and LGI4 interact with ADAM22 and related ADAMs, ADAM11 and ADAM23. The interaction between LGIs and ADAMs is not a simple one to one relationship and is more complicated than we expected. To understand the physiological roles of LGI-ADAM system, examinations of the cell-type specific expression and cell-type specific transcript variants of each gene would be essential.

ACKNOWLEDGMENT

We would like to thank Professor Akinori Akaike (Kyoto University), Kappei Tsukahara, Takashi Seiki and Junro Kuromitsu (Eisai Co., Ltd.) for critical discussions and comments. We also thank Masami Date and Shizuka Ishikawa for their excellent technical assistance.

CONFLICT OF INTEREST

The authors have declared no conflict of interest exists.

REFERENCES

1. Seals DF, Courtneidge SA. The ADAMs family of metalloproteases: multidomain proteins with multiple functions. Genes Dev. 2003; 17(1): 7-30.
2. Blobel CP. ADAMs: key components in EGFR signalling and development. Nat Rev Mol Cell Biol. 2005; 6(1): 32-43.
3. White JM. ADAMs: modulators of cell-cell and cell-matrix interactions. Curr Opin Cell Biol. 2003; 15(5): 598-606.
4. Huovila AP, Turner AJ, Pelto-Huikko M, et al. Shedding light on ADAM metalloproteinases. Trends Biochem Sci. 2005; 30(7): 413-22.
5. Yang P, Baker KA, Hagg T. The ADAMs family: coordinators of nervous system development, plasticity and repair. Prog Neurobiol. 2006; 79(2): 73-94.
6. Sagane K, Ohya Y, Hasegawa Y, et al. Metalloproteinase-like, disintegrin-like, cysteine-rich proteins MDC2 and MDC3: novel human cellular disintegrins highly expressed in the brain. Biochem J. 1998; 334 (Pt 1): 93-8.
7. Sagane K, Yamazaki K, Mizui Y, et al. Cloning and chromosomal mapping of mouse ADAM11, ADAM22 and ADAM23. Gene. 1999; 236(1): 79-86.
8. Takahashi E, Sagane K, Oki T, et al. Deficits in spatial learning and motor coordination in ADAM11-deficient mice. BMC Neurosci. 2006;7:19.
9. Takahashi E, Sagane K, Nagasu T, et al. Altered nociceptive response in ADAM11-deficient mice. Brain Res. 2006; 1097(1): 39-42.
10. Sagane K, Hayakawa K, Kai J, et al. Ataxia and peripheral nerve hypomyelination in ADAM22-deficient mice. BMC Neurosci. 2005; 6(1): 33.
11. Mitchell KJ, Pinson KI, Kelly OG, et al. Functional analysis of secreted and transmembrane proteins critical to mouse development. Nat Genet. 2001; 28(3): 241-9.
12. Godde NJ, D'Abaco GM, Paradiso L, et al. Differential coding potential of ADAM22 mRNAs. Gene. 2007; 403(1-2): 80-8.
13. Ishihama Y, Oda Y, Tabata T, et al. Exponentially modified protein abundance index (emPAI) for estimation of absolute protein amount in proteomics by the number of sequenced peptides per protein. Mol Cell Proteomics. 2005; 4(9): 1265-72.
14. de Godoy LM, Olsen JV, de Souza GA, et al. Status of complete proteome analysis by mass spectrometry: SILAC labeled yeast as a model system. Genome Biol. 2006; 7(6): R50.
15. Chernova OB, Somerville RP, Cowell JK. A novel gene, LGI1, from 10q24 is rearranged and downregulated in malignant brain tumors. Oncogene. 1998; 17(22): 2873-81.
16. Kalachikov S, Evgrafov O, Ross B, et al. Mutations in LGI1 cause autosomal-dominant partial epilepsy with auditory features. Nat Genet. 2002; 30(3): 335-41.
17. Senechal KR, Thaller C, Noebels JL. ADPEAF mutations reduce levels of secreted LGI1, a putative tumor suppressor protein linked to epilepsy. Hum Mol Genet. 2005; 14(12): 1613-20.
18. Fukata Y, Adesnik H, Iwanaga T, et al. Epilepsy-related ligand/receptor complex LGI1 and ADAM22 regulate synaptic transmission. Science. 2006; 313(5794): 1792-5.
19. Schulte U, Thumfart JO, Klocker N, et al. The epilepsy-linked Lgi1 protein assembles into presynaptic Kv1 channels and inhibits inactivation by Kvbeta1. Neuron. 2006; 49(5): 697-706.
20. Kim E, Sheng M. PDZ domain proteins of synapses. Nat Rev Neurosci. 2004; 5(10): 771-81.
21. Novak U. ADAM proteins in the brain. J Clin Neurosci. 2004; 11(3): 227-35.

22. Goldsmith AP, Gossage SJ, ffrench-Constant C. ADAM23 is a cell-surface glycoprotein expressed by central nervous system neurons. J Neurosci Res. 2004; 78(5): 647-58.
23. Bermingham JRJr, Shearin H, Pennington J, et al. The claw paw mutation reveals a role for Lgi4 in peripheral nerve development. Nat Neurosci. 2006; 9(1): 76-84.
24. Katayama H, Tabata T, Ishihama Y, et al. Efficient in-gel digestion procedure using 5-cyclohexyl-1-pentyl-beta-D-maltoside as an additive for gel-based membrane proteomics. Rapid Commun Mass Spectrom. 2004; 18(20): 2388-94.
25. Rappsilber J, Mann M, Ishihama Y. Protocol for micro-purification, enrichment, pre-fractionation and storage of peptides for proteomics using StageTips. Nat Protoc. 2007; 2(8): 1896-906.
26. Ishihama Y, Rappsilber J, Andersen JS, et al. Microcolumns with self-assembled particle frits for proteomics. J Chromatogr A. 2002; 979(1-2): 233-9.